European Radiology (2020) 30:5805–5814
https://doi.org/10.1007/s00330-020-06989-1

MAGNETIC RESONANCE

Evaluation of chronic carotid artery occlusion by non-contrast 3D-MERGE MR vessel wall imaging: comparison with 3D-TOF-MRA, contrast-enhanced MRA, and DSA

Jin Zhang[1] · Shenghao Ding[2] · Huilin Zhao[1] · Beibei Sun[1] · Xiao Li[1] · Yan Zhou[1] · Jieqing Wan[2] · Andrew J. Degnan[3,4,5] · Jianrong Xu[1] · Chengcheng Zhu[6]

Received: 19 March 2020 / Revised: 17 April 2020 / Accepted: 27 May 2020 / Published online: 11 June 2020

Abstract

Objectives To analyze the accuracy of a non-contrast MR vessel wall imaging technique, three-dimensional motion-sensitized driven equilibrium prepared rapid gradient echo (3D-MERGE) for diagnosing chronic carotid artery occlusion (CCAO) characteristics compared with 3D time-of-flight (TOF) MRA, and contrast-enhanced MRA (CE-MRA), using digital subtraction angiography (DSA) as a reference standard.

Methods Subjects diagnosed with possible CCAO by ultrasound were retrospectively analyzed. Patients underwent 3.0-T MR imaging with 3D-MERGE, 3D-TOF-MRA, and CE-MRA followed by DSA within 1 week. Diagnostic accuracy of occlusion, occlusion site, and proximal stump condition were assessed independently on 3 MRI sequences and DSA. Agreement of the above indicators was evaluated in reference to DSA.

Results One hundred twenty-four patients with 129 suspected CCAO (5 with bilateral occlusions) met the inclusion criteria for our study. 3D-MERGE demonstrated a sensitivity, specificity, and accuracy of 97.0%, 86.7%, and 94.6%, respectively, with excellent agreement (Cohen's κ = 0.85; 95% CI, 0.71, 0.94) for diagnosing CCAO in reference to DSA. 3D-MERGE was superior in diagnosing CCAO compared with 3D-TOF-MRA (Cohen's κ = 0.61; 95% CI, 0.42, 0.77) and similar to CE-MRA (Cohen's κ = 0.93; 95% CI, 0.86, 1.00). 3D-MERGE also had excellent agreement compared with DSA for assessing occlusion sites (Cohen's κ = 0.85; 95% CI, 0.71, 0.97) and stump condition (Cohen's κ = 0.83; 95% CI, 0.71, 0.94). Moreover, 3D-MERGE provided additional information regarding the occluded segment, such as distal lumen collapse and vessel wall lesion components.

Conclusion 3D-MERGE can reliably assess chronic carotid occlusive characteristics and has the ability to identify other vessel wall features of the occluded segment. This non-contrast MR vessel wall imaging technique is promising for assessment of CCAO.

Key Points

- *Excellent agreement was found between 3D-MERGE and DSA for assessing chronic carotid artery occlusion, occlusion site, and proximal stump condition.*

Jin Zhang and Shenghao Ding contributed equally to this work and are co-first authors.

✉ Huilin Zhao
huilinzhao2013@163.com

✉ Jianrong Xu
renjixjr@163.com

[1] Department of Radiology, Renji Hospital, School of Medicine, Shanghai Jiaotong University, Shanghai, China

[2] Department of Neurosurgery, Renji Hospital, School of Medicine, Shanghai Jiaotong University, Shanghai, China

[3] Department of Radiology, Perelman School of Medicine at the University of Pennsylvania, Philadelphia, PA, USA

[4] American Institute for Radiologic Pathology, Silver Spring, MD, USA

[5] Department of Radiology, Children's Hospital of Philadelphia, Philadelphia, PA, USA

[6] Department of Radiology, University of Washington, Seattle, WA, USA

• *3D-MERGE was shown to be a more accurate and efficient tool than 3D-TOF-MRA to detect the characteristics of the occluded segment.*
• *3D-MERGE provides not only luminal images for characterizing the proximal characteristics of occlusion but also vessel wall images for assessing the distal lumen and morphology of occlusion segment, which might help clinicians to optimize the treatment strategy for patients with chronic carotid artery occlusion.*

Keywords Carotid artery diseases · Arterial occlusive diseases · Magnetic resonance imaging · Digital subtraction angiography

Abbreviations

3D-MERGE	Three-dimensional motion-sensitized driven equilibrium prepared rapid gradient echo
3D-TOF-MRA	Three-dimensional time-of-flight magnetic resonance angiography
CCA	Common carotid artery
CCAO	Chronic carotid artery occlusion
CE-MRA	Contrast-enhanced magnetic resonance angiography
CPR	Curved planar reconstruction
CTA	Computed tomographic angiography
DSA	Digital subtraction angiography
ICA	Internal carotid artery
MIP	Maximum intensity projection
MRA	Magnetic resonance angiography
MRI	Magnetic resonance imaging
SI	Signal intensity
SNR	Signal-to-noise ratio

Introduction

Carotid artery occlusion (CAO) contributes to approximately 6 to 20% annual risk of recurrent ipsilateral ischemic stroke [1]. Population studies estimate the prevalence of symptomatic CAO at 6/100,000 [2, 3]; when considering transient symptomatic and asymptomatic patients who forgo evaluation or are unaware of chronic carotid artery occlusion (CCAO), the prevalence of CCAO is thought to be significantly greater [3]. CCAO is usually defined as occlusion lasting more than 4 weeks [4]. The optimal treatment of these patients with CCAO is still unclear. Recently, endovascular treatment such as recanalization of CCAO has been reported to be technically feasible but remains challenging. Some studies suggest that stump type, length, and components of the occlusive segment are closely associated with the success rate of recanalization [5–7]. A systematic preprocedural evaluation is therefore important to identify patient and lesion characteristics that carry higher success rates, and thus are helpful for the dissemination of this procedure.

Currently, commonly used imaging methods for diagnosis of CCAO rely on conventional ultrasonography, CT angiography (CTA), MR angiography (MRA), and digital subtraction angiography (DSA) [8]. Ultrasound is a convenient, fast, and cost-effective method for screening CCAO, but has limited arterial coverage and is dependent on the operators' experience. Although CTA and contrast-enhanced MRA (CE-MRA) show high accuracy for detection of CCAO [9], the use of contrast media has a risk of allergic reactions. Time-of-flight (TOF) MRA is commonly used to visualize the carotid arteries without intravenous contrast medium but may overestimate severe luminal stenosis caused by flow artifacts [10, 11]. DSA remains the reference standard for the diagnosis of carotid occlusive disease due to its high resolution, real-time imaging, vascular pathway mapping, and interventional capability at the time of diagnosis [8]. However, none of the above techniques can directly visualize both the residual lumen and the arterial wall of the occluded segment with large coverage.

Recently, rapid three-dimensional MR vessel wall imaging techniques have been developed to visualize arterial lumen and outer wall boundaries non-invasively and without contrast administration [12, 13]. 3D motion-sensitized driven equilibrium prepared rapid gradient echo (3D-MERGE) stands out from various vascular imaging methods of delineating the arterial wall structure [14, 15] due to its excellent suppression of blood signals. Studies have validated the reliability and advantages of 3D-MERGE in assessing carotid atherosclerotic segments [16, 17]. However, few studies have focused on whether the information provided by 3D-MERGE is useful for diagnosis and preoperative evaluation of revascularization. In this study, we sought to assess the accuracy of the 3D-MERGE technique for diagnosing CCAO compared with 3D-TOF-MRA, CE-MRA, and DSA.

Materials and methods

Study population

This study was approved by the institutional review board of Renji Hospital. Informed consent was obtained from all patients prior to enrollment. Patients diagnosed as having CCAO in at least one carotid artery by ultrasound and who were scheduled for intra-arterial DSA between January 2015 and December 2018 were consecutively recruited in this study. All patients underwent carotid multi-contrast MR imaging and DSA within 1 week. Exclusion criteria included (1) surgical history on the index artery, including stenting, endarterectomy, or any other surgery which would affect the normal

structure of the carotid artery; (2) contraindications to MRI or DSA; and (3) acute or chronic renal insufficiency.

Carotid MR imaging

Carotid MR imaging was performed on a 3.0-T whole-body MR scanner (Philips Achieva TX) with a dedicated 8-channel phased-array carotid artery coil (Chenguang). After scout and localization images, a multi-contrast carotid MR imaging protocol was conducted to acquire 3D-TOF-MRA, 3D-MERGE, and CE-MRA centered on the carotid bifurcation. The unenhanced 3D-TOF-MRA was performed with repetition time (TR)/echo time (TE) 20/4 ms, flip angle 20°, field of view (FOV) 88 [FH] × 170[RL] × 170[AP] mm^3, slice thickness 1 mm, 48 slices, and a total acquisition time 4 min 25 s. 3D-MERGE sequence [16] was subsequently performed with repetition time (TR)/echo time (TE) 9.3/4.4 ms, field of view (FOV) 250 [FH] × 160[RL] × 64[AP] mm^3, acquisition matrix size 312 × 200 × 80, spatial resolution 0.8 × 0.8 × 0.8 mm^3, reconstruction resolution 0.4 × 0.4 × 0.4 mm^3, flip angle 6°, and an acquisition time 2 min 42 s. CE-MRA was then performed during the first pass of intravenous injection of a gadolinium contrast agent (Magnevist, Bayer Healthcare) at a dose of 0.1 mmol/kg and a rate of 1.5 mL/s with TR/TE 4.06/1.33 ms, FOV 380 mm × 225 mm, acquisition matrix 384 × 205, slice thickness 1 mm, and duration 20 s.

Carotid DSA

All conventional intra-arterial DSA studies were performed by a neurosurgeon (S. Ding) with 10 years of neurointerventional experience, on a digital angiography unit (Innova 4100; GE Healthcare). After local anesthesia, a 5-F catheter was used to reach the target common carotid artery via a 5-F sheath. Carotid angiography was performed at multiple angles including anterior-posterior and lateral projections. A contrast agent (Iopamiro; Bracco Sine Pharmaceutical) with 370 mg iodine per milliliter was injected 7–8 mL at a flow of 5 mL/s. The digital flat panel pixel matrix was 1000 × 1000 and with a spatial resolution of 0.4 × 0.4 mm^2. Before DSA, patients with ischemic symptoms were prescribed aspirin 100 mg, clopidogrel 75 mg daily, and atorvastatin 20 mg every night. To asymptomatic patients, aspirin 100 mg daily and atorvastatin 20 mg every night were given. At the same time, blood pressure, glucose level, low-density lipoprotein, and other risk factors of all patients were monitored and adjusted to suitable levels for the DSA examination.

Image analysis

DSA images were interpreted by two interventional neuroradiologists (S. Ding and J. Wan with 10 and 15 years of experience in interventional neuroradiology, respectively) who were blinded to MR images at the workstation (AW4.6; GE Healthcare). The MR images were imported to the same workstation used for the DSA interpretation and stripped of patient information, and the image viewer was automatically set a default window/level for the best display. Two radiologists (J. Zhang and H. Zhao with 3 and 9 years of experience in neurovascular MR diagnosis, respectively) reviewed the 3D-MERGE, 3D-TOF-MRA, and CE-MRA images as three separate reading sessions. Analysis of 3D-MERGE was performed on curved planar reconstruction (CPR), and analysis of 3D-TOF-MRA and CE-MRA was performed on maximum intensity projection (MIP) reconstructions. The observers were allowed to adjust the angle or projection to best display the characteristics of the occluded segment. Image quality for 3D-MERGE, 3D-TOF-MRA, and CE-MRA images was independently rated on a 3-point scale [16]: grade 1, excellent, high signal-to-noise ratio (SNR) without artifacts, well-defined vessel wall and lumen margins; grade 2, appropriate for diagnosis, marginal SNR, identifiable wall structures, but partially obscured lumen and vessel wall boundaries; and grade 3, inadequate for diagnosis, low SNR, and obscured arterial wall or vessel boundaries. Arteries with the image quality of grade 3 were excluded from the final analysis.

CCAO was defined as follows: bright blood lumen was closed up or blocked off on 3D-TOF-MRA, black blood lumen was closed up or blocked off on 3D-MERGE, lumen with contrast enhancement media was closed up or blocked off on CE-MRA or DSA. For each CCAO, the following variables were assessed on DSA and corresponding MR images: (a) occlusion site, site of total occlusion was classified into the common carotid artery (CCA), internal carotid cervical segment (C1), petrous segment (C2), and lacerum segment (C3) and above [18]; (b) proximal stump condition, total occlusion lesions of which the occluded proximal sites at the C1 segment were classified into tapered stump, blunt stump, and no stump [5].

In addition, the following variables were assessed on 3D-MERGE images: (a) presence of high signal intensity (SI) in the occluded segment, interpretation of SI was made via reference to the immediately adjacent sternocleidomastoid muscle[19]; (b) distal true lumen visibility, defined as true lumen visibility in the distal area of the occluded lesion; (c) occlusion with full collapse, occlusions with or without full collapse were distinguished by a threadlike or more normal distal lumen by CPR image assessment [20].

Statistical analysis

All statistical calculations were conducted using SPSS software, version 22.0. Categorical variables were summarized by count (percentage). Cohen's κ with 95% CI was used to analyze the inter-reader reproducibility in identifying CCAO, occluded site, and proximal stump condition. In case of

disagreement between the two reviewers, a third reviewer (J. Xu with more than 20 years of experience in neurovascular MR diagnosis) was consulted for final consensus interpretation. The performance of 3D-MERGE, 3D-TOF-MRA, and CE-MRA in diagnosing CCAO was summarized by sensitivity, specificity, positive predictive value, negative predictive value, accuracy, and Cohen's κ with 95% CI using DSA as the criterion standard. Agreement for the occlusion site and proximal stump condition between 3D-MERGE and DSA was quantified by Cohen's κ. A value of Cohen's κ greater than 0.80 was used to indicate excellent agreement and a value between 0.61 and 0.80 to indicate substantial agreement. A p value of less than 0.05 was defined as significant, and all p values were two-sided.

Results

The patient selection flow chart is shown in Fig. 1. Of the 140 recruited patients, 132 underwent DSA within 1 week after the carotid MR imaging, which included 3D-MERGE, 3D-TOF-MRA, and CE-MRA sequences. Two subjects with a history of carotid interventional surgery and 6 subjects with poor MR image quality were excluded. This yielded a total of 124 subjects with 129 suspected CCAO arteries (5 of 124 patients with bilateral occlusion) for the final analysis. Of the 124 patients, 87.9% (109/124) were males, the mean age was 62.0 ± 9.6 years (range, 26 to 81 years), 93.5% (116/124) experienced symptoms for less than 3 months, 60.5% (75/124) had a history of hypertension, 35.5% (44/124) had diabetes, and 34.7% (43/124) had hyperlipidemia.

Inter-reader agreement on DSA, 3D-MERGE, 3D-TOF-MRA, and CE-MRA Images

Inter-reader reproducibility (Cohen's κ; 95% CI) was excellent for diagnosing CCAO by DSA (0.98; 0.92, 1.00), 3D-MERGE (0.91; 0.81, 0.98), and CE-MRA (0.96; 0.89, 1.00), and substantial by 3D-TOF-MRA (0.70; 0.51, 0.85). Inter-reader reproducibility was excellent (all Cohen's $\kappa > 0.80$) for determining occluded site and proximal stump condition by DSA and MR imaging sequences, respectively, as Table 1 shows.

Comparison between MR imaging sequences and DSA for diagnosing CCAO

Agreement values for the qualitative analysis between MR imaging modalities and DSA are summarized in Table 2. Of the 129 suspected CCAO arteries, 99 were diagnosed as true occlusion on DSA images. 3D-MERGE, 3D-TOF-MRA, and CE-MRA detected 96, 94, and 98 of them, yielding sensitivities of 97.0%, 94.9%, and 99.0%, and specificities of 86.7%, 60.0%, and 93.3%, respectively. Compared with the results for 3D-TOF-MRA, the agreements between the other two MR imaging modalities (3D-MERGE and CE-MRA) and DSA showed excellent agreement, with Cohen's $\kappa > 0.80$. Assessments on 3D-TOF-MRA showed the largest variance (Cohen's $\kappa = 0.61$; 95% CI, 0.42, 0.77) compared with assessments on 3D-MERGE (Cohen's $\kappa = 0.85$; 95% CI, 0.71, 0.94) and CE-MRA (Cohen's $\kappa = 0.93$; 95% CI, 0.86, 1.00).

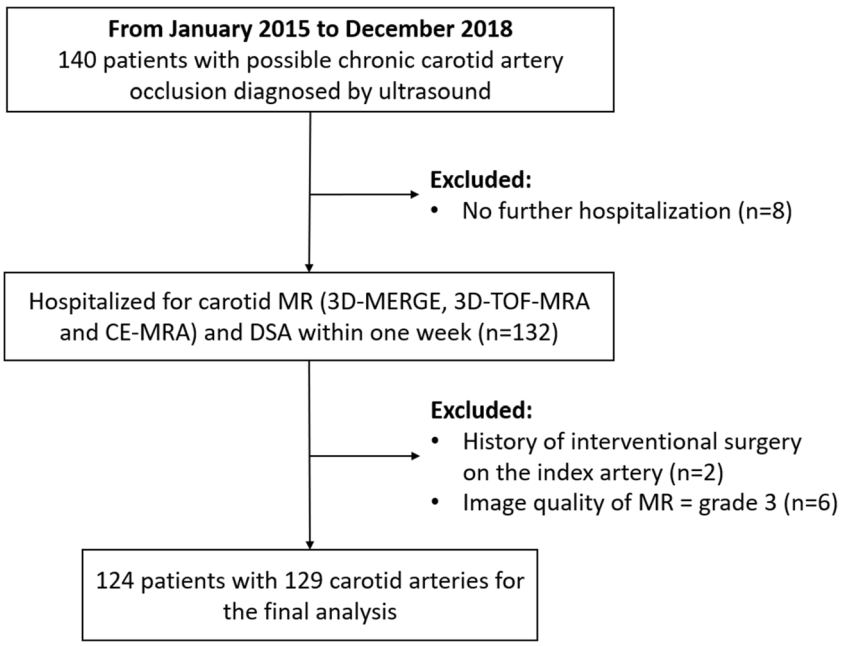

Fig. 1 Flow chart showing the inclusion of patient selection criteria

Table 1 Inter-reader agreement on DSA, 3D-MERGE, 3D-TOF-MRA, and CE-MRA

	DSA	3D-MERGE	3D-TOF-MRA	CE-MRA
CCAO	0.98 (0.92, 1.00)	0.91 (0.81, 0.98)	0.70 (0.51, 0.85)	0.96 (0.89, 1.00)
Occluded site	0.94 (0.86, 1.00)	0.90 (0.80, 1.00)	0.87 (0.74, 0.97)	0.92 (0.81, 1.00)
Proximal stump condition	0.98 (0.94, 1.00)	0.96 (0.89, 1.00)	0.89 (0.78, 0.97)	0.98 (0.94, 1.00)

Numbers out and in parentheses are Cohen's κ value and 95% CIs, respectively

Sample patient images are shown in Fig. 2, indicating that 3D-TOF-MRA is limited as a means of diagnosing CCAO due to intraluminal high SI lesion (Fig. 2), while 3D-MERGE characterizes the geometry nicely.

Comparison between 3D-MERGE and DSA for identifying occlusion sites with CCAO

Table 3 summarizes the results for 3D-MERGE and DSA in identifying the occlusion site for 96 CCAOs diagnosed by both 3D-MERGE and DSA. The sensitivity and specificity of 3D-MERGE for identifying the occlusion site were as follows: CCA, 100.0% and 100.0%; C1, 100.0% and 96.2%; C2, 50.0% and 50.0%; C3 and above, 66.7% and 100.0%, respectively. The Cohen's κ value of the occlusion site obtained by 3D-MERGE and DSA was 0.85 (95% CI, 0.71, 0.97), corresponding to excellent agreement. 3D-MERGE correctly classified all the cases occluded from CCA and C1 segments. However, 3D-MERGE partially misjudged 5 cases where occlusion started from the C2 segment or above (Fig. 4a, b).

Comparison between 3D-MERGE and DSA for proximal stump condition assessment

Cases with CCAO-consistent diagnosis on 3D-MERGE and DSA at C1 segment were compared for proximal stump condition assessment. 3D-MERGE correctly estimated 77.4% (24/31) tapered stumps, 96.6% (28/29) blunt stumps, and 100.0% (15/15) no stump, and shown an excellent agreement with DSA (Cohen's κ = 0.83; 95% CI, 0.71, 0.94) (Table 4; Figs. 3 and 4c, d).

Additional CCAO information provided by 3D-MERGE

The prevalence of additional occlusion characteristics based on stump conditions evaluated by 3D-MERGE is detailed in Table 5. 42.7% (32/75) were found to have high SI lesions in the occluded segment, which may indicate the intraplaque hemorrhage or intraluminal thrombus (Fig. 2b, f), and 61.3% (46/75) were found to have occlusion with full collapse and 74.7% (56/75) to have distal true lumen visibility (Fig. 3j) in the CCAOs at C1 segment. Meanwhile, the presence of high SI, distal true lumen visibility, and occlusion with full collapse were found to be most common in the group of no stump.

Discussion

This study investigated the agreement between 3D-MERGE and conventional angiography techniques including 3D-TOF-MRA and CE-MRA in diagnosing CCAO using DSA as the criterion standard. We found that 3D-MERGE was in close agreement with CE-MRA and demonstrated superior accuracy to 3D-TOF-MRA for diagnosing CCAO. Compared with DSA, we found that 3D-MERGE showed excellent agreement in identification of occluded sites and proximal stump conditions (all Cohen's $\kappa > 0.80$) in CCAO arteries. Moreover, 3D-MERGE provided additional information regarding the occluded segment, such as distal true lumen visibility, collapse, and vessel wall lesion components. To the best of our knowledge, this is the first study to validate 3D-MERGE against the gold standard, DSA, for occluded carotid artery assessments. Our results support the usefulness of 3D-MERGE for CCAO clinical assessment.

Table 2 Comparison between MR imaging sequences and DSA for diagnosing CCAO

	3D-MERGE	3D-TOF-MRA	CE-MRA
Sensitivity	97.0 (90.8, 99.2)	94.9 (88.1, 98.1)	99.0 (94.0, 99.9)
Specificity	86.7 (68.4, 95.6)	60.0 (40.8, 76.8)	93.3 (76.5, 98.8)
Positive predictive value	96.0 (89.5, 98.7)	88.7 (80.7, 93.8)	98.0 (92.3, 99.7)
Negative predictive value	89.7 (71.5, 97.3)	78.3 (55.8, 91.7)	96.6 (80.4, 99.8)
Accuracy	94.6 (89.0, 97.5)	86.8 (79.8, 91.7)	97.7 (93.1, 99.5)
Cohen's κ value	0.85 (0.71,0.94)	0.61 (0.42, 0.77)	0.93 (0.86, 1.00)

All data, except for Cohen's κ value, are percentages. Numbers in parentheses are 95% CIs

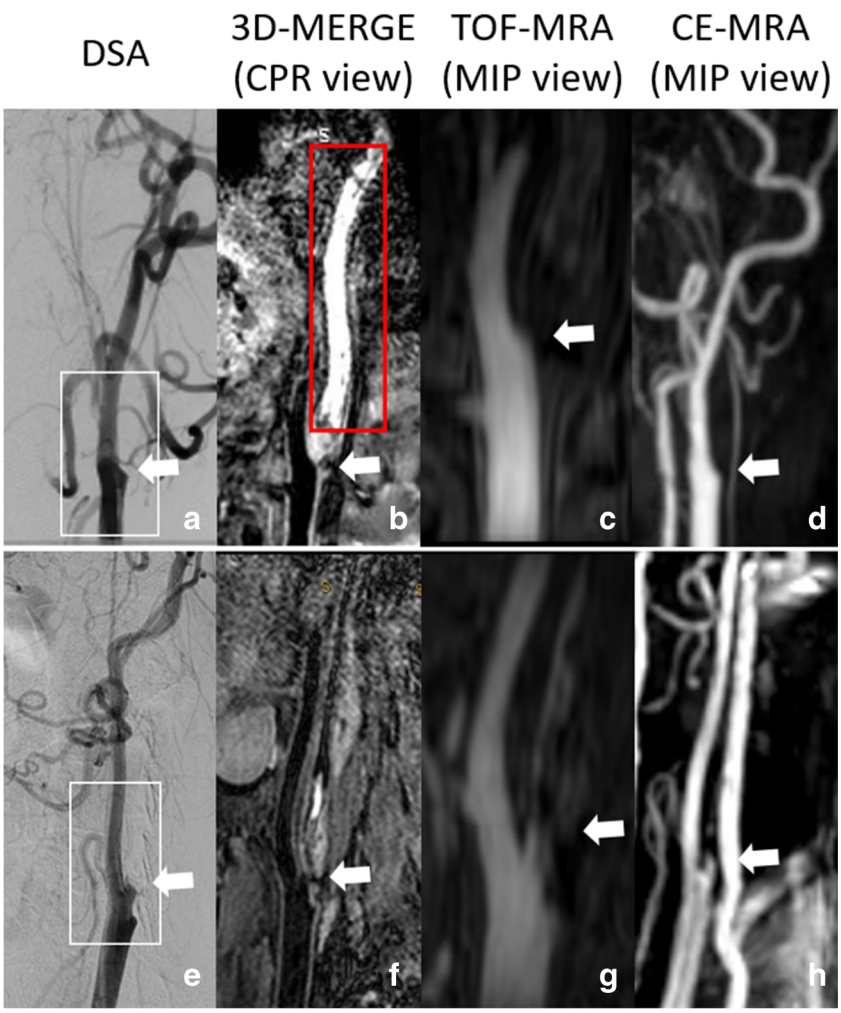

Fig. 2 Comparison between MR imaging sequences and DSA for distinguishing occlusion types. White frames show the coverage of 3D-TOF-MRA in the series of pictures. **a**–**d** Images are from the same CCAO of a 54-year-old man. Arrows show the occlusion at the bifurcation, red frame shows the long segment lesion with high signal intensity (possible thrombus) on 3D-MERGE. **e**–**h** Images are from the same CCAO of a 60-year-old man. The CCAO was misjudged as high-grade stenosis only on 3D-TOF-MRA due to high signal intensity lesion (possible intraluminal thrombus or intraplaque hemorrhage)

When compared with conventional MRA modalities, including 3D-TOF-MRA and CE-MRA, non-contrast 3D-MERGE demonstrated similar agreement, sensitivity, and specificity with CE-MRA and was superior to 3D-TOF-MRA in diagnosing CCAO using DSA as the reference. The main limitation of CE-MRA is the use of gadolinium-based contrast media, dependence on timing of contrast administration which may lead to venous contamination, and risk of renal fibrosis [21]. Compared with non-contrast 3D-TOF-MRA, 3D-MERGE has the following advantages. Firstly, 3D-MERGE is inherently blood-suppressed and insensitive to flow artifacts, while 3D-TOF-MRA is a flow-dependent technique which tends to overestimate the high-grade stenosis as CCAO. Secondly, intraplaque hemorrhage (IPH) or intraluminal thrombus appears as high SI on 3D-TOF-MRA image and may be easily confused with the residual bright blood lumen. In contrast, lumen signal appears negative and vessel wall signal appears positive on the 3D-MERGE images, which achieves high lumen-to-wall contrast [12]. Lastly, 3D-TOF-MRA acquisition with only 48 slices at 1-mm slice thickness takes 4 min 25 s in this study, substantially more than 2 min 42 s for 3D-MERGE with larger anatomic coverage. 3D-MERGE is proven to be a more time-efficient technique than 3D-TOF-MRA in our study.

In this study, 3D-MERGE detected all CCAO originating from CCA and C1 segments with 100% consistency and good morphological comparison with DSA. Our study extends these observations in showing that 3D-MERGE provides

Table 3 Detection of the occlusion site for 96 CCAOs by 3D-MERGE using DSA as reference

Detection by 3D-MERGE	Detection by DSA				
	CCA	C1	C2	C3 and above	Total
CCA	8	…	…	…	8
C1	…	75	2	1	78
C2	…	…	2	2	4
C3 and above	…	…	…	6	6
Total	8	75	4	9	96

Cohen's κ = 0.85 (95% CI, 0.71, 0.97); *CCA*, common carotid artery

Table 4 Estimation of proximal stump condition of 75 CCAOs starting from C1 segment with 3D-MERGE using DSA as the reference standard

Estimation by 3D-MERGE	Estimation by DSA			
	Tapered stump	Blunt stump	No stump	Total
Tapered stump	24	1	…	25
Blunt stump	7	28	…	35
No stump	…	…	15	15
Total	31	29	15	75

Cohen's κ = 0.83 (95% CI, 0.71, 0.94)

highly accurate assessment of occlusion sites in extracranial carotid arteries. However, 3D-MERGE diagnosed 61.5% (8/13) CCAOs where occlusions started from the C2 segment or above, which was less accurate than that of CCA and C1 segments. The reasons for this discrepancy might be due to (1) DSA is an accurate method for CCAO arteries because it is flow-dependent and can visualize the residual lumen even

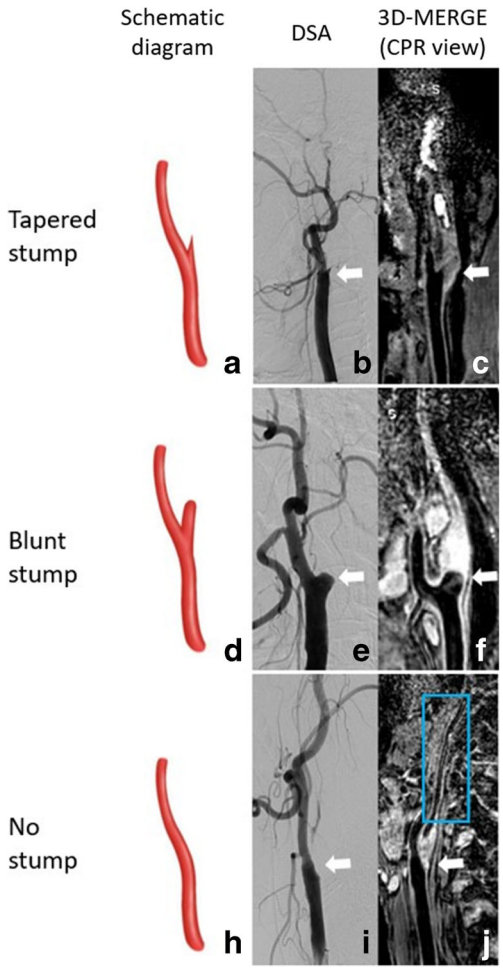

Fig. 3 Proximal stump visualization of CCAO. Arrows show the occlusion sites and proximal stump condition, blue frame shows the thin collapsed lumen distal to CCAO on 3D-MERGE. 3D-MERGE had excellent agreement compared with DSA for assessing occlusion sites and stump condition

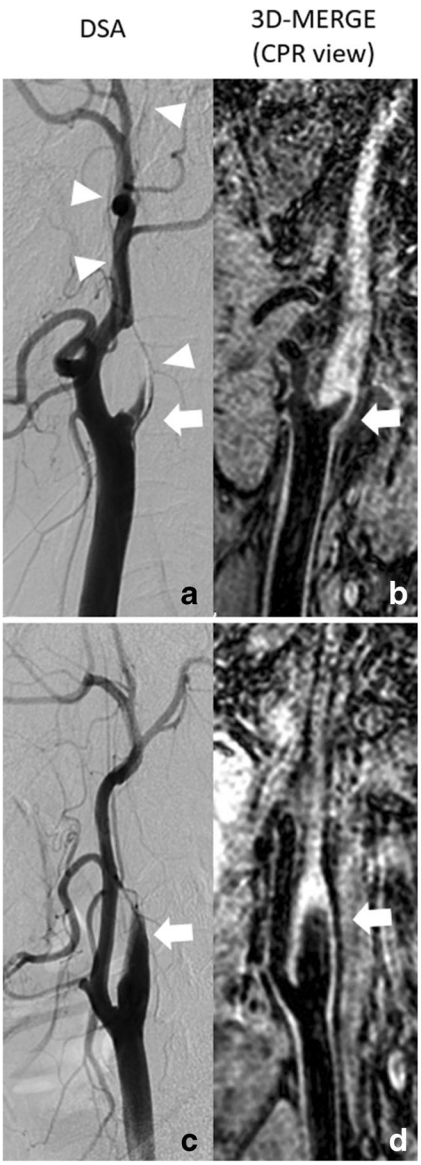

Fig. 4 Cases of misjudgment on 3D-MERGE compared with DSA. **a**, **b** DSA image shows CCAO occludes from C2 segment because of remaining string sign in C1 segment (arrowhead), but CPR image of 3D-MERGE indicates CCAO occludes from the carotid bifurcation (arrow) in a 58-year-old man. **c**, **d** DSA image emerges to a tapered stump (arrow) while CPR image of 3D-MERGE emerges to a blunt stump (arrow) in a 46-year-old woman

Table 5 Prevalence of occlusion characteristics based on stump condition evaluated by 3D-MERGE (n = 75 CCAOs starting from C1 segment)

	Tapered stump (n = 25)	Blunt stump (n = 35)	No stump (n = 15)	Total (n = 75)
Presence of high SI, n (%)	10 (40.0%)	13 (37.1%)	9 (60.0%)	32 (42.7%)
Distal true lumen visibility, n (%)	18 (72.0%)	25 (71.4%)	13 (86.7%)	56 (74.7%)
Occlusion with full collapse, n (%)	13 (52.0%)	22 (62.9%)	11 (73.3%)	46 (61.3%)

with a thin string of slow blood flow, especially for occlusions with upstream long severe stenosis; (2) 3D-MERGE was shown to be limited in identifying the long and thin residual lumen in our study, especially in distal small vessels, because of the much larger voxel size than DSA (0.8 mm vs. 0.4 mm); (3) eccentric flat calcification at proximal occluded sites is sometimes difficult to distinguish from the residual lumen because calcification presents obvious low signal on 3D-MERGE, which is easily confused with the luminal signal [22]; and (4) the method for identifying the location of internal carotid artery segments is not identical between 3D-MERGE and DSA, as 3D-MERGE mainly relies on anatomical landmarks such as the perivascular tissue and the skull [18], whereas DSA relies on the geometry of the internal carotid artery and bony landmarks. We retrospectively analyzed the misjudged cases and found that the occluded sites of 2 arteries were at the junction of C2 and C3 segments.

Proximal stump condition is shown to be closely associated with the success rate of endovascular recanalization [5–7, 23] because it enables the guide wire to go through the true lumen in revascularization. In our study, 3D-MERGE showed excellent agreement with DSA in the detection of stump condition, but 3D-MERGE was found to be not as accurate at detecting tapered stumps as the other methods and accurately diagnosed only 77.4% of the 31 tapered stumps on DSA. We found that minimal distal flow with slow flow or turbulence at the proximal occluded sites might lead to insufficient suppression of blood flow signal on 3D-MERGE. When the tapered stump was relatively narrow and long, the limited voxel size would also interfere with the display of the distal lumen of the stump. Thus, careful attention should be paid when evaluating the tapered stumps on 3D-MERGE images.

The strength of 3D-MERGE should be mentioned in our study. 3D-MERGE provides not only luminal images that can be used for characterizing the proximal characteristics of occlusion but also vessel wall images for assessing the distal lumen and morphology of the occlusion segment. 3D-MERGE can directly display components with different signals in the occlusion and full collapse. High SI lesions in the occlusion may indicate presence of hemorrhage or thrombus, which are prone to rupture and embolization in the endovascular treatment [24–27]. The presence of hemorrhage or thrombus in the occluded segment may also indicate the lesions with lower mechanization or looser texture, compared with the segment with more calcification and fibrous tissue. Occlusion with or without full collapse might relate to hemodynamic mechanisms [28]. Full collapse may indicate insufficient compensation. Visualization of the distal internal carotid artery provides a clear reference for procedures. The above information could not have been provided by conventional MRA or DSA, and is useful for clinical decision and preoperative evaluation. The management of CCAO remains controversial. Although treatment of CCAO is probably not indicated for prevention of embolic events, cerebral hemodynamic and cognitive improvement were reported after successful revascularization of CCAO [29–31]. Development of interventional techniques has made endovascular recanalization of CCAO technically possible. Depending on the lesion characteristics, endovascular recanalization may be useful as a less invasive technique offering similar reperfusion advantages with a lower risk of cranial nerve injury, wound complications, and neck hematoma compared with open surgery [23, 29]. A preprocedural evaluation of CCAO is important to identify lesion characteristics that enable higher success rate of endovascular recanalization versus those lesions that might be inaccessible to endovascular access or otherwise at higher risk of failure. Future clinical decision-making for endovascular recanalization in patients with CCAO should be based not only upon residual lumen features but also upon the intrinsic characteristics of the occluded segment, and evaluation of effective collateral circulation along with high success rate of revascularization may benefit more for patients with CCAO [32].

This study has a few limitations. First, we used a single sequence (3D-MERGE) to assess carotid artery occlusion characteristics. If multi-contrast sequences such as standard T1- and T2-weighted vessel wall imaging are added to the imaging protocol, more information including specific components of occlusion, types of thrombus, and strings of blood flow could be determined. Second, the carotid artery coil only covered from the common carotid artery to the C3 segment of the internal carotid artery in this study. Internal carotid artery portions above the C3 segment and downstream the middle cerebral artery cannot be clearly visualized. Neurovascular coils with larger longitudinal coverage are suggested for future studies.

In conclusion, 3D-MERGE can reliably diagnose CCAO and assess the morphological characteristics of occluded segments in the proximal site. With the advantage of its non-invasive nature, avoiding ionizing radiation exposure and contrast administration, 3D-MERGE is a promising tool for diagnosing CCAO.

Funding information This study has received funding from the grants by the Shanghai Municipal Health Commission Project (201940060), Shanghai Jiao Tong University Project (YG2016MS56), Renji Hospital Project (RJZZ18-002, 2019NYBSZX01), and National Natural Science Foundation of China (81571630; 81801650).

Compliance with ethical standards

Guarantor The scientific guarantor of this publication is Huilin Zhao, MD, PhD.

Conflict of interest The authors of this manuscript declare no relationships with any companies, whose products or services may be related to the subject matter of the article.

Statistics and biometry No complex statistical methods were necessary for this paper.

Informed consent Written informed consent was obtained from all subjects (patients) in this study.

Ethical approval Institutional Review Board approval was obtained.

Methodology
- retrospective
- cross-sectional study
- performed at one institution

References

1. Klijn CJM, Kappelle LJ, Tulleken CAF, Van Gijn J (1997) Symptomatic carotid artery occlusion. A reappraisal of hemodynamic factors. Stroke 28:2084–2093
2. Bryan DS, Carson J, Hall H et al (2013) Natural history of carotid artery occlusion. Ann Vasc Surg 27:186–193
3. Flaherty ML, Flemming KD, McClelland R, Jorgensen NW, Brown RD Jr (2004) Population-based study of symptomatic internal carotid artery occlusion: incidence and long-term follow-up. Stroke 35:e349–e352
4. Iwata T, Mori T, Tajiri H, Miyazaki Y, Nakazaki M (2012) Long-term angiographic and clinical outcome following stenting by flow reversal technique for chronic occlusions older than 3 months of the cervical carotid or vertebral artery. Neurosurgery 70:82–90 discussion 90
5. Chen YH, Leong WS, Lin MS et al (2016) Predictors for successful endovascular intervention in chronic carotid artery total occlusion. JACC Cardiovasc Interv 9:1825–1832
6. Li J, Wang C, Zou S, Liu Y, Qu L (2019) Hybrid surgery for nontaper or nonstump lesions in symptomatic subacute or chronic internal carotid occlusion: a better solution. World Neurosurg 122: e1416–e1425
7. Hasan D, Zanaty M, Starke RM et al (2018) Feasibility, safety, and changes in systolic blood pressure associated with endovascular revascularization of symptomatic and chronically occluded cervical internal carotid artery using a newly suggested radiographic classification of chronically occluded cervical internal carotid artery: pilot study. J Neurosurg. https://doi.org/10.3171/2018.1.JNS172858:1-10
8. Malhotra K, Goyal N, Tsivgoulis G (2017) Internal carotid artery occlusion: pathophysiology, diagnosis, and management. Curr Atheroscler Rep 19:41
9. Kaufmann TJ, Kallmes DF (2005) Utility of MRA and CTA in the evaluation of carotid occlusive disease. Semin Vasc Surg 18:75–82
10. Nederkoorn PJ, Der Graaf YV, Eikelboom BC, Der Lugt AV, Bartels LW, Mali WPTM (2002) Time-of-flight MR angiography of carotid artery stenosis: does a flow void represent severe stenosis? AJNR Am J Neuroradiol 23:1779–1784
11. Weber J, Veith P, Jung B et al (2015) MR angiography at 3 Tesla to assess proximal internal carotid artery stenoses: contrast-enhanced or 3D time-of-flight MR angiography? Clin Neuroradiol 25:41–48
12. Wang J, Yarnykh VL, Yuan C (2010) Enhanced image quality in black-blood MRI using the improved motion-sensitized driven-equilibrium (iMSDE) sequence. J Magn Reson Imaging 31:1256–1263
13. Okuchi S, Fushimi Y, Okada T et al (2019) Visualization of carotid vessel wall and atherosclerotic plaque: T1-SPACE vs. compressed sensing T1-SPACE. Eur Radiol 29:4114–4122
14. Edelman RR, Mattle HP, Wallner B et al (1990) Extracranial carotid arteries: evaluation with "black blood" MR angiography. Radiology 177:45–50
15. Edelman RR, Chien D, Kim D (1991) Fast selective black blood MR imaging. Radiology 181:655–660
16. Zhao H, Wang J, Liu X et al (2015) Assessment of carotid artery atherosclerotic disease by using three-dimensional fast black-blood MR imaging: comparison with DSA. Radiology 274:508–516
17. Murata K, Murata N, Chu B et al (2020) Characterization of carotid atherosclerotic plaques using 3-dimensional MERGE magnetic resonance imaging and correlation with stroke risk factors. Stroke 51: 475–480
18. Bouthillier A, Van Loveren HR, Keller JT (1996) Segments of the internal carotid artery: a new classification. Neurosurgery 38:425–433
19. Yuan C, Mitsumori LM, Ferguson MS et al (2002) In vivo accuracy of multispectral magnetic resonance imaging for identifying lipid-rich necrotic cores and intraplaque hemorrhage in advanced human carotid plaques. Circulation 104:2051–2056
20. Fox AJ, Eliasziw M, Rothwell PM, Schmidt MH, Warlow C, Barnett HJM (2005) Identification, prognosis, and management of patients with carotid artery near occlusion. AJNR Am J Neuroradiol 26:2086–2094
21. Scott LJ (2018) Gadobutrol: a review in contrast-enhanced MRI and MRA. Clin Drug Investig 38:773–784
22. Balu N, Yarnykh VL, Chu B, Wang J, Hatsukami T, Yuan C (2011) Carotid plaque assessment using fast 3D isotropic resolution black-blood MRI. Magn Reson Med 65:627–637
23. Zanaty M, Roa JA, Jabbour PM, Samaniego EA, Hasan DM (2020) Recanalization of the chronically occluded internal carotid artery: review of the literature. World Neurosurg X 5:100067
24. JM UK-I, Fox AJ, Aviv RI et al (2010) Characterization of carotid plaque hemorrhage: a CT angiography and MR intraplaque hemorrhage study. Stroke 41:1623–1629
25. Yuan C, Parker DL (2016) Three-dimensional carotid plaque MR imaging. Neuroimaging Clin N Am 26:1–12
26. McNally JS, McLaughlin MS, Hinckley PJ et al (2015) Intraluminal thrombus, intraplaque hemorrhage, plaque thickness, and current smoking optimally predict carotid stroke. Stroke 46: 84–90
27. Naghavi M, Libby P, Falk E et al (2003) From vulnerable plaque to vulnerable patient: a call for new definitions and risk assessment strategies. Part I. Circulation 108:1664–1672
28. Johansson E, Ohman K, Wester P (2015) Symptomatic carotid near-occlusion with full collapse might cause a very high risk of stroke. J Intern Med 277:615–623
29. Aboyans V, Ricco JB, Bartelink MEL et al (2018) 2017 ESC guidelines on the diagnosis and treatment of peripheral arterial diseases, in collaboration with the European Society for Vascular Surgery (ESVS): document covering atherosclerotic disease of extracranial

carotid and vertebral, mesenteric, renal, upper and lower extremity arteries endorsed by: the European Stroke Organization (ESO) The Task Force for the Diagnosis and Treatment of Peripheral Arterial Diseases of the European Society of Cardiology (ESC) and of the European Society for Vascular Surgery (ESVS). Eur Heart J 39: 763–816

30. Lin MS, Chiu MJ, Wu YW et al (2011) Neurocognitive improvement after carotid artery stenting in patients with chronic internal carotid artery occlusion and cerebral ischemia. Stroke 42:2850–2854
31. Zanaty M, Howard S, Roa JA et al (2019) Cognitive and cerebral hemodynamic effects of endovascular recanalization of chronically occluded cervical internal carotid artery: single-center study and review of the literature. J Neurosurg. https://doi.org/10.3171/2019.1.JNS183337:1-9
32. Lin T, Lai Z, Lv Y et al (2018) Effective collateral circulation may indicate improved perfusion territory restoration after carotid endarterectomy. Eur Radiol 28:727–735